1-1-2008

Expression Patterns of Arabidopsis DRG Genes: Promoter-GUS Fusions, Quantitative RT-PCR and Patterns of Protein Accumulation in Response to Environmental Stresses

Joel P. Stafstrom

Original Citation
Stafstrom, JP (2008). Expression patterns of Arabidopsis DRG genes: Promoter::GUS fusions, quantitative RT-PCR and patterns of protein accumulation in response to environmental stresses. Intl. J. Plant Sci. 169(8):1046–1056.

Int. J. Plant Sci. 169(8):1046–1056. 2008.

1058-5893/2008/16908-0007$15.00 DOI: 10.1086/590443

EXPRESSION PATTERNS OF *ARABIDOPSIS DRG* GENES: PROMOTER-GUS FUSIONS, QUANTITATIVE REAL-TIME PCR, AND PATTERNS OF PROTEIN ACCUMULATION IN RESPONSE TO ENVIRONMENTAL STRESSES

Joel P. Stafstrom[1]

Plant Molecular Biology Center, Department of Biological Sciences, Northern Illinois University, DeKalb, Illinois 60115, U.S.A.

*DRG*s are very highly conserved GTP-binding proteins. All eukaryotes contain *DRG1* and *DRG2* orthologs. *Arabidopsis* has three *DRG*s: *AtDRG1* (At4g39520), *AtDRG2* (At1g17470), and *AtDRG3* (At1g72660). *DRG2* and *DRG3* encode proteins that are 95% identical; identity between *DRG1* and *DRG2/3* is 55%. The focus of this article is expression of *Arabidopsis DRG*s. *DRG1* and *DRG2* promoter-GUS constructs showed similar spatial expression in seedlings and mature organs, but gene-specific differences were noted. Quantitative real-time PCR experiments indicated similar levels of *DRG1* and *DRG2* mRNA accumulation in most tissues. *DRG3* transcripts were very low in all tissues. Heat stress at 37°C led to a 10-fold increase in *DRG1* transcripts and a 1000-fold increase in *DRG3* transcripts. *DRG1* antibodies recognized a 43-kD protein, and *DRG2* antibodies recognized bands at 30, 43, and 45 kD. Plants were exposed to stresses (salt, heat, cold, UV light, osmotic, and other stresses) and examined by Western blotting. Only heat stress caused detectable changes. Heat did not affect *DRG1*, but *DRG2* and a 72-kD protein recognized by *DRG2* antibodies both increased. The modest changes in *DRG* mRNA and protein levels seen here suggest that other types of regulation, such as altered subcellular localization, may be important for their cellular functions.

Keywords: *DRG*, GTPase, GTP-binding protein, heat stress, environmental stress.

Introduction

GTP-binding proteins (G proteins) regulate a wide variety of cellular activities in all organisms (Bourne et al. 1990, 1991; Bischoff et al. 1999; Leipe et al. 2002). Some well-characterized G proteins are Gα of heterotrimeric G proteins, small monomeric G proteins (including Ras, Ran, Rab, Rho, and Arf), several translation initiation and elongation factors (bacterial IF2, EF-G, EF-Tu, and their eukaryotic counterparts), and components of signal-recognition particles and their receptors. Heterotrimeric G proteins are widely used in eukaryotic signal transduction pathways, including those in plants (Jones and Assmann 2004). Ras, which is critical for regulating cell proliferation in animals, is one of the few G proteins that does not occur in plants. ROPs, which are related to Rho G proteins, may carry out Ras-like activities in plants (Yang 2002; Vernoud et al. 2003). Rab proteins provide specificity for vesicle targeting, Rho contributes to organization of the actin cytoskeleton, Ran regulates transport into and out of nuclei, and Arf is involved in vesicle assembly (Bischoff et al. 1999). The functions of many other subfamilies of G proteins remain poorly understood.

The availability of complete genome sequences from a large number of bacteria, archaea, and eukaryotes has led to a better understanding of the origins and evolutionary relationships of GTPases. A thorough phylogenetic analysis was based on the structure of the GTP-binding pocket and of various effector domains (Leipe et al. 2002). The origins of ~10 major G-protein families can be traced to the last universal common ancestor of all living organisms, suggesting that they perform essential physiological activities. Among these 10 families are four translation-factor families, two additional families of predicted translation factors, two signal-recognition particle-associated GTPases, and two OBG-like GTPases, OBG and *DRG*. OBG is an essential gene in *Bacillus subtilis* (Morimoto et al. 2002). Genes for nuclear-encoded OBGs in eukaryotes are presumed to have originated in the bacterial ancestors of mitochondria and chloroplasts. *DRG*s, the focus of this report, occur in archaea and eukaryotes. All 10 ancient families of G proteins associate with ribonucleoprotein complexes and probably play important roles in RNA metabolism in extant cells (Caldon et al. 2001; Leipe et al. 2002).

*DRG*s from archaea and unicellular eukaryotes are assigned to COG 1163 (http://www.ncbi.nlm.nih.gov/COG/). Each archaeal species has a single *DRG* gene, whereas eukaryotes contain members of two orthologous groups, *DRG1* (KOG 1487) and *DRG2* (KOG 1486). All eukaryotes appear to contain at least one representative of each group (Li and Trueb 2000). A mouse *DRG* was the first to be characterized; it is the archetype of the *DRG1* group (Sazuka et al. 1992*a*, 1992*b*). A human *DRG* became the archetype of the *DRG2* group (Schenker et al. 1994). Both *DRG1* and *DRG2* from most organisms contain ~365–370 amino acid residues and have molecular masses of ~43 kDa. Amino acid identity of *DRG*s from plants, animals, and fungi is very high: identity

[1] E-mail: stafstrom@niu.edu.

Manuscript received November 2007; revised manuscript received December 2007.

within an orthologous group is ~65%–70%, whereas paralogs from a single species share ~55%–60% identity. The guanine nucleotide-binding pocket (G1–G5 motifs) of *DRG1* and *DRG2* proteins is contained roughly between residues 60 and 290. The C-terminus contains a TGS domain (pfam02824), which also occurs in threonyl-tRNA synthase and *E. coli* SpoT, and is suggested to be an RNA-binding domain (Wolf et al. 1999).

In *Arabidopsis*, the only *DRG* to be characterized to date is encoded by At1g17470. We previously referred to this protein as *AtDRG* (Devitt et al. 1999), whereas another group called it *AtDRG1* (Etheridge et al. 1999). Based on a more recent naming scheme (Li and Trueb 2000), this gene and its encoded protein will be referred to as *AtDRG2* and *AtDRG2* (or simply *DRG2*), respectively. *Arabidopsis* contains two additional *DRG* genes. The sequence of At4g39520 shows clear affinity with the *DRG1* orthologous group, so it will be called *AtDRG1*. We refer to the last gene, At1g72660, as *AtDRG3*. *AtDRG2* and *AtDRG3* encode proteins containing 399 amino acids that are 95% identical to each other.

Some aspects of *DRG* mRNA and protein accumulation have been studied in several organisms. Two studies on animal *DRG*s are of note because they examined the expression of both *DRG1* and *DRG2* in their respective systems. Li and Trueb (2000) studied steady state levels of both mRNAs by Northern blotting of mouse and human tissues. In mouse, both mRNAs were moderately abundant in testis, kidney, liver, brain, and heart and were reduced or absent in skeletal muscle, lung, and spleen. Both messages were present in 12 human tissues but varied somewhat in abundance. In all cases, though, the relative levels of *DRG1* and *DRG2* mRNAs were similar. In SV40-transformed fibroblasts, *DRG2* levels were low and *DRG1* levels were high, suggesting a compensatory interaction between the expression of these genes (Li and Trueb 2000; see also Schenker et al. 1994). Ishikawa and coworkers (2003) studied the expression of *Xenopus DRG1* and *DRG2* by Northern blotting and in situ hybridization. Both mRNAs accumulated steadily and rather similarly during *Xenopus* development. The exception to this generality was seen at the earliest stages of development, where *XDRG1* was absent and *XDRG2* was moderately abundant. In adult tissues, both messages were moderately abundant in most tissues (*XDRG1* was present at very low levels in heart, lung, and liver) and highly abundant in testis and ovaries. In situ hybridization revealed similar but not identical spatial patterns of expression of these two genes.

Using Northern blots, we previously showed that pea *DRG2* mRNA accumulates preferentially in tissues that are in a growing state (Devitt et al. 1999). We also showed that *Arabidopsis DRG2* expression parallels that of a histone gene, which is a marker for actively dividing and elongating cells (Devitt et al. 1999). We concluded that plant *DRG2* genes are broadly expressed but that there is a somewhat greater level of expression in some growing, dividing, or metabolically active cells and tissues. In yeast two-hybrid assays, human *DRG1* was found to interact with the TAL1/SCL proto-oncoprotein, suggesting a role in cell-cycle control (Mahajan et al. 1996; Zhao and Aplan 1998). Immunolocalization studies of *Arabidopsis DRG2* protein (which the authors called *AtDRG1*) showed that this protein occurs in punctate granules, but the identity of these granules or organelles remains unknown (Etheridge et al. 1999).

In this article, I focus on expression patterns of *Arabidopsis DRG* genes using promoter-GUS fusions involving the *DRG1* and *DRG2* promoter regions (called *prDRG1* and *prDRG2*), transcript accumulation of all three genes using quantitative real-time PCR (qRT-PCR), and protein accumulation on Western blots using *DRG1*- and *DRG2*-specific antibodies.

Material and Methods

Plants

Arabidopsis thaliana, ecotype Wassilewskija (Ws), was used for all experiments. Roots (Rt) and young leaves (YL) were from 2-wk-old plants grown sterilely on vertically oriented MS plates at 25°C under continuous light. For all other tissues, plants were grown in ProMix in a growth chamber at 20°C. To examine the effects of photoperiod, plants first were grown for 25 d under short-day photoperiods (SD; 10L : 14D). Some plants were then transferred to long-day photoperiods (LD; 16L : 8D). SD and LD samples were collected after a total of 28 d. All other tissues were collected from SD plants, including old rosette leaves (OL) from 6-wk-old plants, inflorescence stems (St), flower buds (Bd), open flowers (Fl), and green siliques (Si). To test for response to various environmental stresses, seeds were sown on horizontal MS agar plates, cold treated at 4°C in the dark for 3 d, and then grown for 9–10 d in a growth chamber at 25°C in continuous light. Plants then were exposed to a particular agent for 6 or 24 h. For chemical treatments, 85-mm round plates were flooded with 10 mL of solution. Plants were kept in the growth chamber during the treatment periods, except for temperature treatments at 4° or 37°C, which were carried out in a dark refrigerator or incubator, respectively. Both dark and light controls were performed. The treatments tested were UV light (a single exposure of 10^5 μJ delivered using a Stratagene Stratalinker); 275 mM mannitol; 25 μM ethidium bromide; 100 mM NaCl; 100 μM glyphosate; 1 mM $NaAsO_2$ (arsenite); 1 mM Na_2HAsO_4 (arsenate); and 100 mM K-phosphate at pH 4.4, 5.6, 7.4, and 8.8. Tissues for qRT-PCR and Western blots were frozen in liquid nitrogen and stored at −80°C.

Cloning, Sequencing, and Construction of GUS Constructs

Work on the *DRG2* promoter predated the availability of *Arabidopsis* genomic sequence. A previously described *DRG2* cDNA clone (Devitt et al. 1999) was used to screen the CD4–8 genomic library in the λ-Fix vector (obtained from the Arabidopsis Biological Resource Center [ABRC]). We isolated and fully sequenced a clone containing an insert of ~5 kb, which included ~1.6 kb of DNA upstream of the ATG start codon. Four regions of the *DRG2* promoter region were amplified by PCR and cloned into the *Agrobacterium* binary vector pBI101. Sequences of the PCR primers were F1 (within λ-Fix), GTCCTGCAGCCACACATGAGGAATACC; F2, TAGGTCGACGTGTAGTGAGCAAGGCTAGAG; R1, CGCGGATCCGGCGAAGAGAGGG; and R2, CGCGGATCCTTCACTTGTTTTTGCTAC (restriction sites added for cloning are underlined). The following primer pairs were used

to produce four *DRG2* promoter constructs: construct I, F1 and R2; construct II, F2 and R2; construct III, F1 and R1; and construct IV, F2 and R1 (see fig. 1). These clones were transformed into *Agrobacterium* strain GV3101, and the resulting cells were used to transform Ws *Arabidopsis* plants by vacuum infiltration (Bechtold and Pelletier 1998). Kanamycin-resistant plants were selected on MS plates, tested for the presence of the appropriate DNA by PCR, and brought to homozygosity.

The *DRG1* promoter region was cloned based on the published genomic sequence. Sequences of the forward and reverse primers were TGTGTCGACTGGTTAATATCGAGAAGCTGAAGG and ACTCCATGGTTGCAGTCAAAGCACAG, respectively. These primers amplified a 628-bp fragment, which was cloned into binary vector pCAMBIA 1382. This clone was transformed into *Agrobacterium* strain GV3101, which was used to transform Ws *Arabidopsis* plants by the floral dip method (Clough and Bent 1998). Hygromycin-resistant plants were selected on MS plates, tested for the presence of the appropriate DNA by PCR, and brought to homozygosity.

Histochemical detection of GUS activity was carried out by incubating plants or plant parts for 4–18 h in 0.5 mM X-gluc (5-bromo-4-chloro-3-indolyl-β-D-glucopyranoside) in a buffer containing 50 mM Na-phosphate, pH 7.0, and 0.1% Triton X-100 (Jefferson et al. 1987; Beeckman and Engler 1994). Chlorophyll was cleared through several changes of 70% ethanol. Digital images were captured directly with a camera or with a light microscope using brightfield or darkfield optics.

Antisera and Western Blotting

DRG2 antibodies (antiserum no. 55) were generated by immunizing rabbits with a His-tagged fusion protein containing the N-terminal 202 residues of pea *DRG2* (Devitt et al. 1999). The entire 369-residue coding region of At*DRG1* was cloned into pQE30 (Qiagen) in order to generate a fusion protein containing a His-tag at its N-terminus. Forward and reverse PCR primers corresponding to the *AtDRG1* cDNA were used to amplify the entire coding region (AGAGGATCCATGTCGACTATTATGCAGAAG and CATGGTACCTCATATCTTTTTAACGATCTGAACAAC, respectively). A cDNA clone was used as a template (clone M70O01 in pBlueScript SK$^-$ from ABRC). Rabbits were immunized by injecting antigen into surgically implanted ball chambers (Clemons et al. 1992). *DRG1* antibodies (antiserum no. 29) were affinity purified using an AffiGel-10 column (BioRad) to which *DRG1*-His had been covalently bound.

Proteins were extracted by grinding in extraction buffer on ice (50 mM Tris-HCl, pH 7.5, 100 mM NaCl, 2 mM EDTA, 29 mM β-mercaptoethanol, and 2 mM phenylmethylsulfonyl fluoride). Protein concentrations were determined using a dye-binding assay (BioRad). Polyacrylamide gel electrophoresis (SDS-PAGE) was performed on 10% or 12% acrylamide gels using standard techniques. In a given experiment, either 50 or 100 μg of protein was loaded in each lane. Equal loadings were verified by staining identical gels with Coomassie brilliant blue (these control gels are not shown). Proteins were

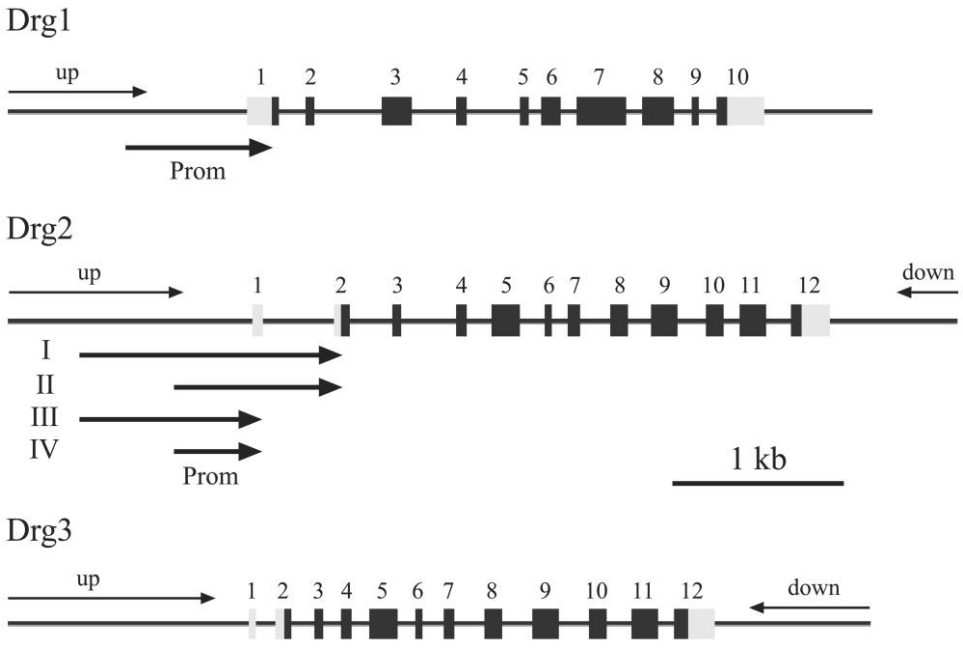

Fig. 1 Structure of *Arabidopsis DRG1*, *DRG2*, and *DRG3* genes. *DRG1* encodes a predicted protein containing 369 residues with a mass of 41.1 kDa. *DRG2* and *DRG3* encode proteins containing 399 amino acids with masses of ~44.6 and 44.8 kDa, respectively. The sizes and positions of coding exons of *DRG2* and *DRG3* are identical (coding exons are shown in black and noncoding exons are shown in gray). Exon 1 and intron 1 of *DRG2* and *DRG3* are within the 5′ noncoding regions of these genes. The "up" and "down" arrows indicate the limits of the coding regions of upstream and downstream genes (arrowheads show the positions of stop codons). Upstream promoter regions of *DRG1* and *DRG2* (*Prom*) were fused to β-glucuronidase (GUS) to make transcriptional fusions. One promoter construct was generated for *DRG1*, and four constructs were made for *DRG2*.

electrophoretically transferred to nitrocellulose or polyvinylidene difluoride membrane blots using a semidry apparatus. Blots were incubated overnight in Tris-buffered saline (TBS; 20 mM Tris, pH 7.5, 500 mM NaCl) with affinity-purified primary antibodies at dilutions ranging from 1 : 100 to 1 : 1000. Following washes in TBST (TBS plus 0.05% Tween-20), blots were incubated for 1–2 h with HRP-DAR secondary antibodies in TBS at a dilution of 1 : 5000 (donkey-antirabbit antibodies conjugated to horseradish peroxidase, Amersham). A second series of washes in TBST ensued. Finally, blots were incubated in SuperSignal West Pico chemiluminescence substrate (Pierce) and exposed to x-ray film.

Quantitative Real-Time PCR

Total cellular RNA was purified using the RNAqueous-4PCR kit together with Plant RNA Isolation Aid (both from Ambion). Residual genomic DNA was hydrolyzed by DNAase treatment. Reverse transcription was carried out using the RETROscript kit (Ambion). The resulting cDNAs were used as templates for qRT-PCR.

In most cases, each primer spanned two exons, and there was at least one additional exon within the amplicon. Exon structure of three *DRG* genes is summarized in figure 1. The coding sequences of *DRG2* and *DRG3* are very similar, so forward primers for these genes were based on 5′ noncoding sequences (in each of these genes, exon 1 and intron 1 are wholly contained within 5′ noncoding DNA). The sequences of these primers were *DRG1qF* (spans exons 2 and 3), CTTCTCATCATCTGGGTTTGTTAAAGGCCAAGCTTGCTAAGC; *DRG1qR* (spans exons 5 and 6), TGCATGTCCTAGCCGTACTTATAACCTGTCTTCCTCTACCTTTTC; *DRG2qF* (spans exons 1 and 2), CGGAGATCGCCCTTCACCAATTCCACTATAGTAGCAAAAACAAG; *DRG2qR* (spans exons 4 and 5), GACTTTCCGACACTAGGAAATCCTATAAGTGCAACACGTC; *DRG3qF* (spans exons 1 and 2), CGGTAGACAATCGATGCCAAAGTGTGAAGATACCTCAGTC; and *DRG3qR* (within exon 4), CCCATACTTTGTAACTTCAAAACCATCCCCACCTCCACTAG. The actin-8 gene (At1g49240) was used as an internal control. Primers for this gene were Actin8F, TCAGCACTTTCCAGCAGATG, and Actin8R, ATGCCTGGACCTGCTTCAT. For end-point PCR, *DRG* gene-specific primers were used to amplify cDNA templates for 40 amplification cycles at an annealing temperature of 65°C. The products were electrophoresed on agarose gels and visualized by ethidium bromide fluorescence. To verify the identity of these PCR products, bands were isolated from the gels, cloned into pGEM-T-Easy (Promega), and sequenced.

Quantitative RT-PCR reactions were carried out in an Mx3000P real-time PCR system (Stratagene). A master mix was prepared using 1.25 μL each of forward and reverse primers, each at 10 ng/μL, 6.75 μL water, and 0.25 μL of a 100× dilution of reference dye R4526 (Sigma). For each reaction, 9.5 μL of the mastermix, 3 μL of an appropriate template (water or cDNA), and 12.5 μL of SYBR Green JumpStart Taq ReadyMix (Sigma S4438) were mixed in a final volume of 25 μL. Negative controls included a no-template control (water) for each primer pair to measure interference due to primer-dimer formation and a DNAase-treated RNA control to assess contamination from genomic DNA. The standard cycling conditions were as follows: denaturation (94°C for 2 min) was followed by 40 cycles of amplification (94°C for 30 s, 60°C for 30 s, 72°C for 30 s) and final extension (72°C for 1 min). Data were collected at the end of each annealing step. The cycle threshold (Ct) for each sample was generated by MxPro software. The Ct value for each sample corresponded to the point at which the fluorescence crossed the threshold. Fluorescence from SYBR Green increases as double-stranded DNA accumulates (Morrison et al. 1998). Following amplification, characterization of products was performed by melting-curve analysis (95°C for 1 min, 55°C for 30 s, 95°C for 30 s). Fluorescence data were continuously collected as the temperature ramped up from 55° to 95°C. The dissociation curve for each sample was generated by MxPro software to determine the melting temperature (T_m) of the reaction product or products using the value $-Rn'(T)$, which is the first derivative of the normalized fluorescence reading multiplied by −1. Relative expression data presented here are normalized to 10,000 actin transcripts. Replicate experiments showed similar results.

Results

Structure of Arabidopsis DRG *Genes*

The *Arabidopsis* genome contains three *DRG* genes, which we refer to as *DRG1* (At4g39520), *DRG2* (At1g17470), and *DRG3* (At1g72660). The positions and sizes of introns, exons, 5′ and 3′ untranslated regions (UTRs), ORF limits of upstream and downstream genes, and other features are shown in figure 1. *DRG1* encodes a protein of 369 amino acid residues. *DRG2* and *DRG3* encode proteins containing 399 residues. Overall amino acid identity between *DRG1* and *DRG2*/*DRG3* is ~56%, whereas identity between *DRG2* and *DRG3* is 95%. Canonical GTP-binding domains include five G boxes and two switch regions. These motifs all occur between residues 80 and 290 of each *DRG* protein. A TGS domain, which may be involved in RNA binding, spans residues 290–365. *DRG* proteins from nearly all organisms contain ~365–370 residues. A 32-amino-acid "tail" at the C-terminus of *Arabidopsis DRG2* and *DRG3* also occurs in pea *DRG2* (GenBank AF014821). The coding region of *DRG1* contains 10 exons. *DRG2* and *DRG3* each contain 12 exons. Exon 1 and intron 1 of these two genes are wholly contained within their 5′ UTRs.

Promoter Constructs and Expression

Upstream promoter regions of *DRG1* and *DRG2* were fused with β-glucuronidase (GUS) to make transcriptional fusions. Several attempts also were made to generate transgenic plants expressing the *DRG3* promoter fused with GUS. Although hygromycin-resistant plants were isolated, none of these showed reliable GUS expression in any tissue or in response to heat stress. The λ CD4–8 genomic library was screened using a *DRG2* cDNA as a probe. The largest clone isolated was ~5.0 kb, including ~1.6 kb of DNA upstream of the ATG start codon. This clone was fully sequenced (J. P. Stafstrom, unpublished data). Exon 1 of *DRG2* was 74 bp in length. Four promoter constructs were generated by PCR and then cloned into pBI101. These constructs contained either 982 or 448 bp of DNA upstream of exon 1, either with or without intron 1 (427 bp; fig. 1). Transgenic plants were generated that contained each promoter construct. GUS expression

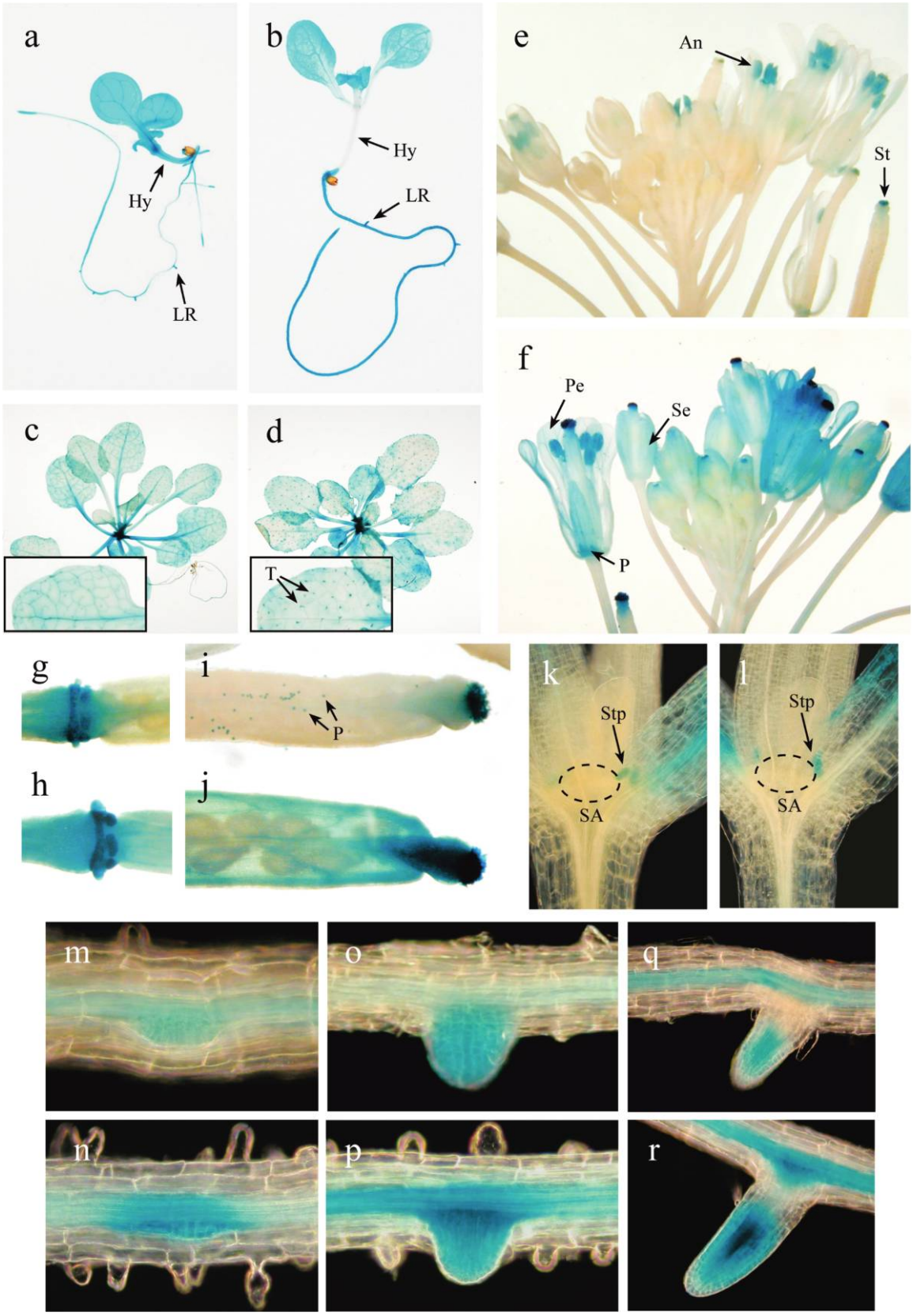

Fig. 2 Expression in *Arabidopsis* tissues of *DRG1* and *DRG2* promoter-GUS transcriptional fusions. GUS activity was assayed in transgenic plants containing fusions to *prDRG1* (*a*, *c*, *e*, *g*, *i*, *k*, *m*, *o*, *q*) or *prDRG2* (*b*, *d*, *f*, *h*, *j*, *l*, *n*, *p*, *r*). Tissues analyzed were 7-d-old seedlings (*a*, *b*),

was not detected from promoter constructs that lacked the intron (constructs III and IV; data not shown). Expression from constructs I and II was strong in many tissues, and spatial and temporal expression patterns appeared to be identical (data not shown). It is now apparent that construct II begins near the stop codon of the upstream gene and that construct I extends into that gene (fig. 1). All data shown below are from the longest construct, construct I. A single *prDRG1*-GUS construct was generated in pCAMBIA 1382 based on the *Arabidopsis* genomic sequence. This promoter region contained 628 bp of DNA immediately upstream of the ATG start codon.

Expression of *prDRG1*-GUS and *prDRG2*-GUS was examined in cells and tissues throughout the plant life cycle. In general, both promoters were active at many stages of development. In seedlings, *prDRG1* was strongly expressed in cotyledons, hypocotyls, and roots, particularly at the root apex and in lateral root primordia (fig. 2*a*). *prDRG2* was expressed in the blades of cotyledons and was strongly expressed in roots, but it was not expressed in hypocotyls or the petioles of cotyledons (fig. 2*b*). Rosette leaves of plants grown in short photoperiods expressed both genes (fig. 2*c*, 2*d*). However, *prDRG1* was more strongly expressed in vascular tissues and *prDRG2* was quite specifically expressed in trichomes (fig. 2*c*, 2*d*, insets). Inflorescences contain flowers at progressive stages of development. *prDRG1* was expressed predominantly in anthers and stigmas (fig. 2*e*). Much or all of the "anther staining" is due to staining of pollen within these anthers (pollen staining is seen more clearly in fig. 2*i*). *prDRG2* also was expressed strongly in anthers and stigmas and, in addition, it was expressed in sepals and petals (fig. 2*f*). Both genes were expressed in the receptacle regions of older flowers, particularly in abscission scars of sepals, petals, and stamens (fig. 2*g*, 2*h*). *prDRG2* was expressed in silique walls (fig. 2*j*), whereas *prDRG1* was not expressed in these walls (fig. 2*i*). Examination of the shoot apex region of young seedlings by darkfield microscopy was able to reveal staining throughout the depths of these tissues. Expression of both genes occurred in stipules at the bases of leaf primordia, but there was no apparent expression in the shoot apical meristem (fig. 2*k*, 2*l*). At low magnification, expression of both genes in roots appeared to be uniform (fig. 2*a*, 2*b*). A closer examination of roots using darkfield microscopy showed that the *DRG1* and *DRG2* promoters were more active in vascular cells than in the cortex or epidermis (fig. 2*m*, 2*n*). Both genes were expressed in pericycle cells as they were undergoing periclinal divisions to produce new lateral roots (fig. 2*m*, 2*n*). High levels of expression persisted as new root apical meristems were organized and emerged through the cortex (fig. 2*o*, 2*p*). As roots grew further, expression remained high in their meristems but diminished in more mature cells between the apex and the parent root (fig. 2*q*, 2*r*).

Transgenic plants expressing promoter-GUS constructs were grown on MS plates to test for responses to environmental stresses. These included 200 mM NaCl; 20% PEG8000 and mannitol at 3%, 6%, and 10% (osmotic stress); 4°C; 37°C; H_2O_2 at 10 mM and 100 mM (oxidative stress); and desiccation (15 or 30 min of air from a small fan blown over uncovered plates). None of these treatments led to noticeable changes in the amount or localization of GUS staining in *prDRG1* or *prDRG2* plants (data not shown).

Quantitative Real-Time PCR

Gene-specific primers were designed to carry out qRT-PCR for each *DRG* gene (see "Material and Methods" for details). Several precautions were taken to ensure that quantitative data were due to amplification of a specific gene and of cDNA derived from mRNA, not genomic DNA. Total RNA, which was used to produce cDNA by reverse transcription, was treated with DNAase to destroy genomic DNA. Also, primers were designed to include at least one exon within the amplicon that was not complementary to the primers. Complementary DNAs prepared from several tissues were subjected to nonquantitative end-point PCR (fig. 3). In every case, only a single band was amplified by each pair of primers. The size of each PCR product was identical to the size that would be amplified from cDNA. Finally, an example of each band was subcloned into pGEM-T-Easy and sequenced. Each sequence exactly matched that of the expected cDNA (data not shown).

Complementary DNAs isolated from several tissues were used as templates for quantitative RT-PCR (fig. 4). Melting-curve analysis of each transcript indicated the presence of a single species, which is further evidence for the specificity of these reactions (data not shown). Replicate experiments gave the same results. Transcript numbers were normalized to actin-8 transcripts (Ct values relative to 10,000 actin transcripts). In each tissue, the levels of *DRG1* and *DRG2* transcripts were similar. A comparison between tissues indicated a range of ~10-fold in the levels of each of these two transcripts, with roots and stems containing relatively low levels and flower buds, open flowers, and green siliques containing relatively high levels. *DRG3* transcripts could be detected in most tissues, but their levels were ~30-fold to 100-fold lower than those of *DRG1* or *DRG2*.

Western Blotting

Patterns of *DRG1* and *DRG2* protein accumulation were analyzed on Western blots using specific, affinity-purified antisera. *DRG2* antibodies recognized protein bands with apparent molecular masses of 45, 43, and 30 kDa (fig. 5). The amount of each band was variable in different tissues. The smaller bands are proteolytic products of the 45-kDa band (B. Nelson, K. Maas, J.-M. Dekeyser, and J. Stafstrom, unpublished manuscript). In control experiments, *DRG2* antibodies barely recognized *DRG1*-His (not shown). *DRG1* antibodies are highly specific for *DRG1*, which has an apparent molecular mass of 43 kDa. Portions of the same batches of tissues that were analyzed by qRT-PCR (fig. 4) were used to prepare

6-wk-old rosettes grown in short photoperiods (*c*, *d*; insets show details of single leaves), inflorescences (*e*, *f*), receptacle regions following organ abscission (*g*, *h*), silique wall and stigma (*i*, *j*), shoot apex region of young seedlings (*k*, *l*), and seedling roots at various stages of lateral root development (*m*–*r*). Identified structures or organs are anther (*An*), hypocotyl (*Hy*), lateral root (*LR*), pollen (*P*), petal (*Pe*), shoot apex (*SA*), sepal (*Se*), stipule (*Stp*), stigma (*St*), and trichome (*T*).

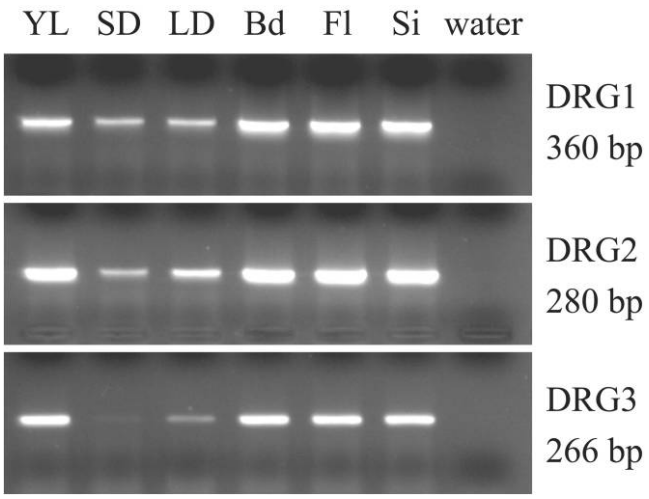

Fig. 3 End-point PCR using qRT-PCR primers using gene-specific PCR primers. Complementary DNAs prepared from young leaves (*YL*), leaves of 4-wk-old plants grown under short (*SD*) or long (*LD*) photoperiods, flower buds (*Bd*), open flowers (*Fl*), and green siliques (*Si*) were used as templates for standard PCR reactions. Water was used as a negative control. An agarose gel stained with ethidium bromide is shown. Each pair of primers produced a single band of the expected size. Sequencing one band of each type confirmed its identity.

protein samples for Western blot analysis (fig. 5). The levels of *DRG1* in each tissue were quite similar, although noticeably lower levels were present in siliques and leaves of SD and LD plants. *DRG2* levels were considerably more variable. The 45-kDa band was highly abundant only in flower buds, whereas the 43-kDa band was present in roots, stems, young leaves, flower buds, and open flowers. Low levels of the 30-kDa band were present in stems, flower buds, and open flowers. Very little (if any) of the three *DRG2* bands was detected in old leaves, leaves of SD or LD plants, or siliques.

Accumulation of *DRG* proteins in response to a variety of chemicals and to alterations of the physical environment were examined (fig. 6). Samples were collected from seedlings grown on agar plates after 6 or 24 h of treatment. The 30-kDa *DRG2* band was not present in any sample, so this region of the blots is not shown. Since some treatments occurred in the dark and others in the light, controls under both conditions were performed. The presence or absence of light did not affect accumulation of either protein (fig. 6*a*). In fact, none of the treatments tested had a large effect on the accumulation of the 43-kDa *DRG1* band or the 43/45-kDa *DRG2* bands. These treatments included exposure to 4°C, UV light, mannitol, ethidium bromide, NaCl, glyphosate, Na-arsenite, Na-arsenate, or pH over the range of 4.4–8.8. An exception was the response of *DRG2* to heat stress at 37°C. Heat stress led to an increase of the 45-kDa band at 6 h, and it also led to the appearance of a 72-kDa protein that was recognized by *DRG2* antibodies (fig. 6*a*). A time-course experiment showed that increased accumulation of the 45- and 72-kDa bands begins 3 h after the onset of heat stress (fig. 6*b*). These bands persisted at elevated levels through 24 h of continuous heat stress. During recovery from heat stress (6 h at 37°C, followed by a return to 25°C), the 72-kDa band was still present after 6 h (6 + 6 sample) but was gone after 24 h (6 + 24 sample).

DRG *mRNA Expression in Response to Heat Stress*

Accumulation of *DRG* transcripts in response to heat stress was examined by qRT-PCR (fig. 7). During exposure to heat stress at 37°C, *DRG2* transcript levels declined about eightfold over 24 h. In contrast, *DRG1* transcripts increased about eightfold during the first 3 h of heat stress and then declined gradually to their initial levels by 24 h. *DRG3* transcripts, which were barely detectable in tissues grown under normal conditions, increased more than 1000-fold within 3 h of the onset of heat stress. Accumulation of *DRG* transcripts during recovery from heat stress was also examined (fig. 7). Plants first were exposed to 37°C for 3 h and then allowed to recover at 25°C. Following 3 h of recovery (3 + 3 samples), *DRG2* transcript levels were unchanged (cf. the 3-h sample), *DRG1* transcripts declined slightly, and *DRG3* transcript levels declined ~10-fold. At later recovery stages (3 + 9 and 3 + 21 samples), the level of each transcript changed little from the 3 + 3 stage. Heat treatments occurred in a dark incubator. The 0 + 24 sample was a control that was kept in the dark but was not subjected to heat stress.

Discussion

Very little is known about the cellular functions of *DRG1* or *DRG2* from any organism. It is also unknown whether they perform similar functions. This is quite surprising given the very high level of sequence conservation among *DRG*s and the many important functions performed by other types of G proteins. An understanding of where and when these genes are

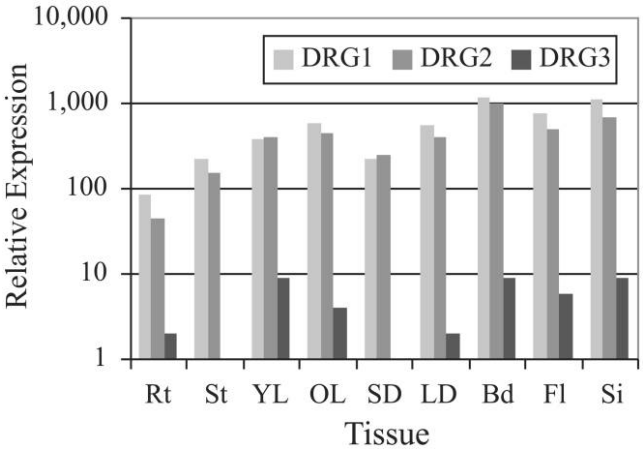

Fig. 4 qRT-PCR analysis of *DRG* transcripts from *Arabidopsis* tissues. Complementary DNAs were prepared from the same six tissues shown in fig. 3 as well as from roots (*Rt*), stems (*St*), and old leaves (*OL*). The actin-8 gene was used as an internal control for quantitative comparisons. Relative expression values based on measured cycle threshold values were normalized to 10,000 actin transcripts. In each of these tissues, there were similar levels of *DRG1* and *DRG2* transcripts. Between tissues, the transcript levels varied by up to 10-fold (e.g., roots vs. flower buds). *DRG3* mRNA was present at very low but detectable levels in most tissues.

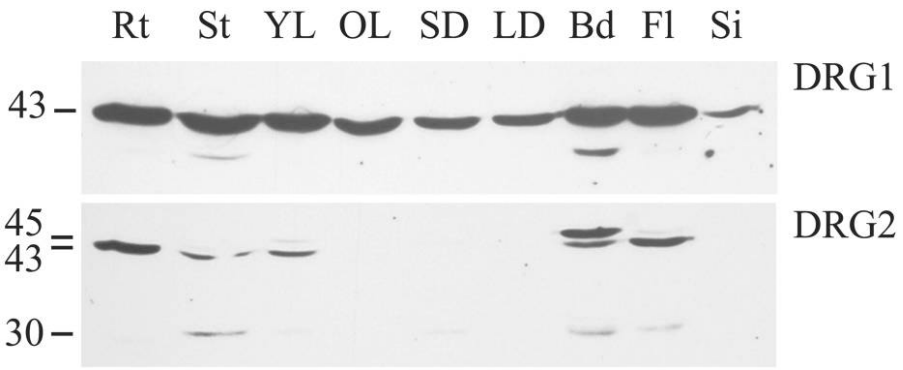

Fig. 5 Patterns of *DRG* protein accumulation in *Arabidopsis* tissues. Western blots were probed with *DRG1*- or *DRG2*-specific, affinity-purified rabbit antibodies. The tissues analyzed were identical to those examined by qRT-PCR (see fig. 4). *DRG1* antibodies recognized a single band at 43 kDa. *DRG2* antibodies recognized three forms of *DRG2* at 45, 43, and 30 kDa. *DRG1* was present at similar levels in all of these tissues. The amount of each form of *DRG2* was variable. All three *DRG2* bands were nearly undetectable in old rosette leaves, rosette leaves from long- and short-photoperiod plants, and siliques.

expressed and how this expression is controlled by internal and external factors could reveal aspects of their function. Also, such information would certainly provide a vital foundation for ongoing biochemical, cellular, and genetic studies.

In this study, expression patterns of *Arabidopsis DRG* genes were examined using three approaches. Each approach can provide useful information, but each has its limitations as well. First, qRT-PCR was used to determine steady state levels of *DRG* mRNAs (figs. 4, 7). Using several types of controls, we established that the Ct threshold values reported were specific to a particular gene. This consideration was especially important for *DRG2* and *DRG3*, in which the nucleotide sequences of their coding regions were 90% identical. Similar results to those reported here are available from microarray databases. Nevertheless, it is important for individual investigators to repeat these experiments, especially when, for example, relative cellular levels of mRNAs and proteins do not correspond with one another. Second, Western blotting was used to assess *DRG1* and *DRG2* protein levels. *DRG1* antibodies were highly specific for a 43-kDa band and never recognized a 45-kDa band, which is the size of the largest form of *DRG2*. We have established through other work that the 45-, 43-, and 30-kDa bands recognized by *DRG2* antibodies are breakdown products of *DRG2* (B. Nelson, K. Maas, J.-M. Dekeyser, and J. Stafstrom, unpublished manuscript). *DRG2* antibodies recognize *DRG1*-His only very weakly, so the 43-kDa band recognized by these antibodies is predominantly *DRG2*. Our third approach was to generate transgenic plants expressing promoter-GUS transcriptional fusions. This was a very useful adjunct to the other approaches because neither of these could reveal cellular patterns of gene expression. Our focus was on the promoters of *DRG1* (*prDRG1*) and *DRG2* (*prDRG2*), because we were unable to obtain verifiable transgenic plants containing *prDRG3* fused to GUS. Transgenic plants were generated that contained four different *DRG2* promoter constructs fused to GUS (fig. 1). Constructs III and IV lacked intron 1, which is wholly contained within the 5′ UTR. GUS expression was not seen in plants containing these constructs, so cis elements within the intron might be important for high levels of promoter activity. Intron-mediated enhancement of gene expression has been documented for a number of other genes (Callis et al. 1987; Mascarenhas et al. 1990; Rose 2004).

Steady state levels of *DRG1* and *DRG2* mRNAs were similar to each other in all of the tissues that were tested. Also, there was only ~10-fold difference between the tissues with the highest and lowest levels of accumulation of each mRNA (fig. 4). Based on the tissues analyzed, these genes are broadly expressed, a general conclusion that corroborates that of microarray experiments (Craigon et al. 2004; Zimmermann et al. 2004; Schmid et al. 2005). Aliquots of the same tissue samples were used for qRT-PCR (fig. 4) and for Western blotting (fig. 5). The levels of *DRG1* protein were similar in these tissues. In contrast, *DRG2* levels were highly variable: significant amounts of the 45-kDa complete protein were found only in flower buds, and very little of any of the three forms of *DRG2* could be detected in old leaves, plants grown under SD or LD photoperiods, or siliques. Because the *DRG2* mRNA levels in these tissues were very similar (fig. 4), the discrepancy between protein and mRNA accumulation in siliques, old leaves, and leaves of SD and LD plants may be due to differential protein synthesis, degradation, or both within these tissues. We previously noted discrepancies in the relative levels of *DRG2* mRNA and protein in pea axillary buds (Devitt et al. 1999). In this case, however, protein levels were constant, whereas mRNA levels were more abundant in growing buds than in dormant buds. *DRG1* and *DRG2* from *Xenopus*, human, and mouse are susceptible to polyubiquitination and degradation by the 26S proteosome pathway (Ishikawa et al. 2005). Each *DRG* protein is stabilized through an interaction with a specific *DRG* family regulatory protein (DFRP). It is hypothesized that this interaction prevents polyubiquitination. *Arabidopsis* contains DFRP homologues, but it is not known whether they play a similar role in stabilizing *DRG*s.

The very high level of sequence conservation among *DRG*s from eukaryotes and archaea and the quite similar bacterial OBGs suggest that they play an important and perhaps related role in all of these organisms. The broadly similar patterns of mRNA accumulation that we have observed indicate that transcription is not the primary level at which the *DRG*s are regulated. Still, accumulation of *DRG* proteins might vary in

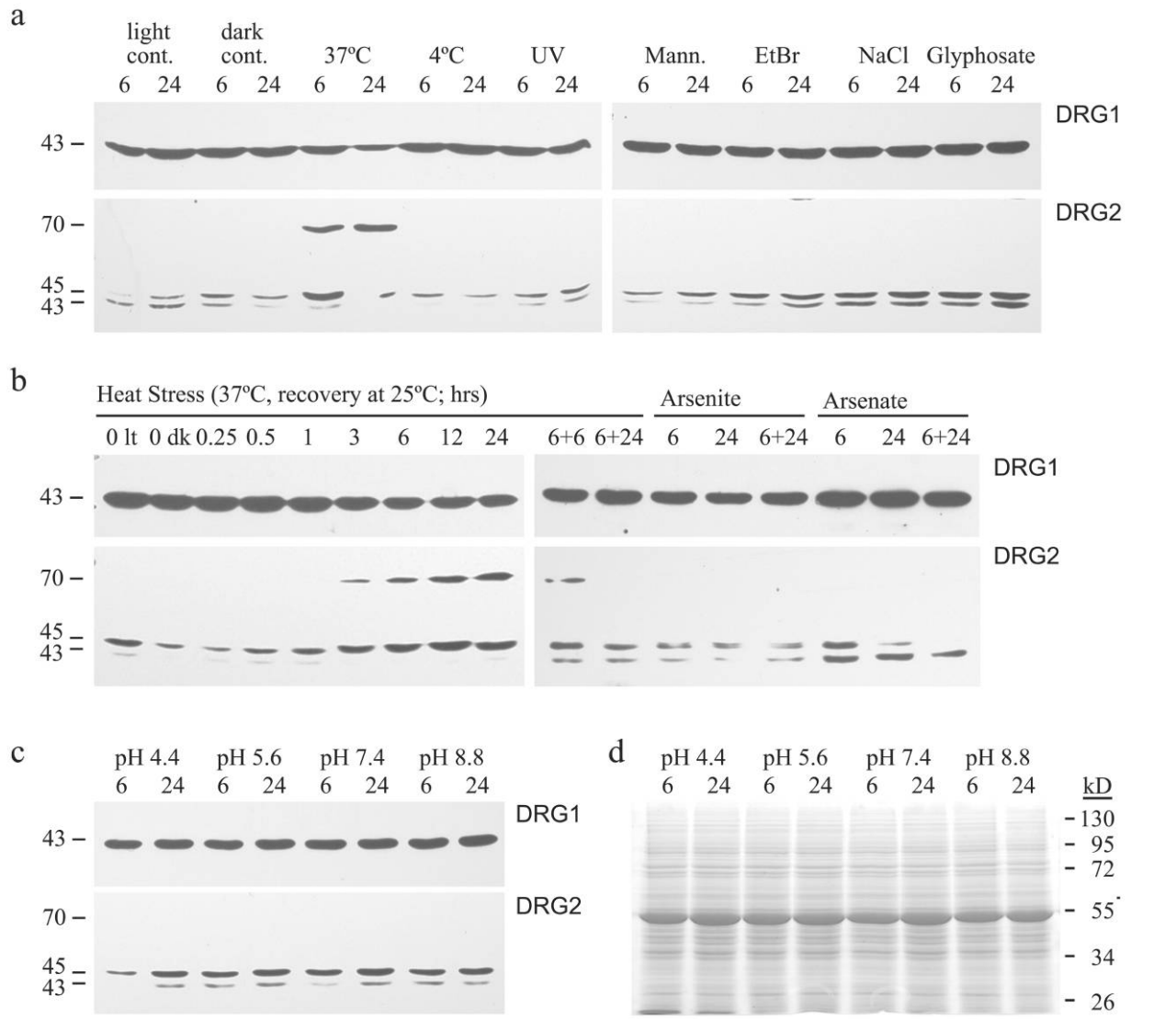

Fig. 6 Patterns of *DRG* protein accumulation in response to chemical and environmental stresses. Plants were grown on MS plates for 9 d. Some treatments were in the light and others were in the dark, so controls for both are included. *a–c*, Plants were exposed to the following conditions and collected 6 or 24 h after the onset of the treatment (treatment was continuous except for UV light): 37°C, 4°C, UV light (single exposure to 10^5 μJ), 275 mM mannitol, 25 μM ethidium bromide, 100 mM NaCl, 100 μM glyphosate, 1 mM Na-arsenite, 1 mM Na-arsenate, and 100 mM K-phosphate at pH 4.4, 5.6, 7.4, or 8.8. The effect of heat stress at 37°C also was analyzed over a time course of 0.25–24 h. Recovery from heat stress at 37°C for 6 h was analyzed after an additional 6 or 24 h at 25°C. Most treatments had little effect on the accumulation of *DRG1* or *DRG2*. Heat stress led to increases in the *DRG2* 45-kDa band and to a 72-kDa band that was recognized by *DRG2* antibodies. The 72-kDa protein appeared within 3 h of the onset of heat stress and persisted through 24 h. This protein was still present following 6 h of recovery at 25°C but was absent after 24 h of recovery. *d*, Example of a Coomassie-stained gel to demonstrate equivalent loadings in all lanes. Samples were identical to those loaded in *c*.

response to some internal or external stimulus, such as a hormone or an environmental stress. We tested a variety of stresses and other treatments using young plantlets grown on MS plates. Experimental parameters (e.g., concentrations, durations of treatments, etc.) were selected based on the *Arabidopsis* Gantlet Project (http://thale.biol.wwu.edu/) and other sources. The conditions we used were generally similar to those published recently by the Harter Laboratory (Kilian et al. 2007). The conditions tested were high and low temperatures, genotoxic stress (UV light and ethidium bromide), osmotic stress (mannitol), salinity, amino acid starvation (glyphosate), arsenate (heavy metal toxicity), arsenite (oxidative stress), and pH over the range of 4.4–8.8 (fig. 6). Most of these treatments had little or no effect on the accumulation of *DRG1* or the 43- and 45-kDa forms of *DRG2*. Furthermore, none of the conditions tested altered GUS expression driven by *prDRG1* or *prDRG2*.

The only treatment that affected *DRG* accumulation patterns was heat stress at 37°C. Exposure to this temperature for 6 h led to increased accumulation of the 45-kDa form of *DRG2*, but *DRG1* was not affected (fig. 6*a*). *DRG3* mRNA

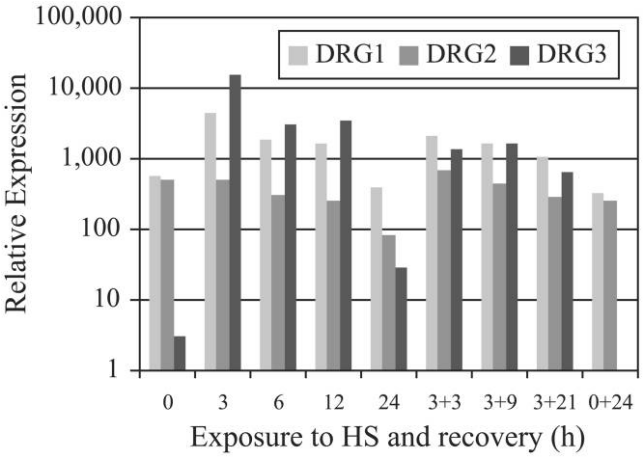

Fig. 7 qRT-PCR analysis of *DRG* transcripts in response to heat stress. Nine-day-old seedlings grown on MS plates were exposed to continuous heat stress at 37°C in the dark for 0, 3, 6, 12, or 24 h. Following 3 h of heat stress, other plants were allowed to recover at 25°C for an additional 3, 9, or 21 h (3 + 3, 3 + 9, and 3 + 21; 0 + 24 is a continuous dark control that was not exposed to heat stress). *DRG2* transcript levels declined in response to heat stress. *DRG1* transcript levels were upregulated about eightfold after 3 h of heat stress; these transcripts gradually declined to starting levels by 24 h. *DRG3* was upregulated ~1000-fold by heat stress. Relative expression values based on measured cycle threshold values were normalized to 10,000 actin transcripts.

was not expressed at significant levels in any tissue (fig. 4), but its abundance increased more than 1000-fold in young plants after 3 h at 37°C (fig. 7). Heat stress also increased *DRG3* mRNA accumulation in microarray experiments (Zimmerman et al. 2004). The accumulation of *DRG1* transcripts was increased by 10-fold by this treatment, but *DRG2* transcripts were unaffected (fig. 7). Response to heat stress might require increased levels of both *DRG1* and *DRG2* proteins; in this case, the need for a *DRG2*-type protein could be fulfilled by *DRG3*, which is 95% identical to *DRG2* at the amino acid level. Heat stress also led to the accumulation of a ~72-kDa protein that was recognized by *DRG2* antibodies (fig. 6). This protein appeared as early as 3 h after the onset of heat stress and persisted at high levels for the duration of this stress (up to 24 h; fig. 6*b*). The 72-kDa protein was still present 6 h after the onset of recovery at 25°C but was gone by 24 h. The identity of this protein is unknown. The temporal pattern of accumulation of the 72-kDa protein parallels that of *DRG3* transcripts. However, both *DRG2* and *DRG3* are predicted to encode proteins of ~45 kDa, and there are no apparent alternative splice sites in either gene that might produce a larger protein. Alternatively, the *DRG2* antibodies might recognize related epitopes in another protein. A BLAST-P search indicated that an OBG-like protein encoded by At5g18570 is the most similar sequence to *DRG2* (other than *DRG1*). This protein is predicted to be targeted to chloroplasts and has a predicted mass of 75.6 kDa, which is quite similar to that of the band that we observed. At5g18570 transcripts do not increase in response to heat stress (Kilian et al. 2007), but its encoded protein might accumulate if it were stabilized by this treatment. Another possibility is that *DRG2* (or *DRG3*) becomes covalently conjugated to another protein, thus increasing its mass. These possibilities might be resolved by purifying the 72-kDa protein and determining its amino acid composition or part of its sequence.

Loss-of-function mutants might be expected to have their strongest effects on the cells in which the genes are normally expressed. Consequently, information about the cell-level expression of *DRG*s will be valuable for our ongoing analyses of *drg* mutants, which include T-DNA insertion lines from the Salk collection and other collections and RNAi mutants. Given that *DRG1* and *DRG2* are broadly expressed and that their encoded proteins are quite similar, single mutants might be complemented during normal development, partially or fully, by the other gene. Since *DRG3* is hardly expressed except in response to heat stress, a mutation in this gene might reveal a phenotype only under stress conditions. Although *prDRG1* and *prDRG2* showed overlapping patterns of activity, some differences were seen: *prDRG1* was more abundantly expressed in hypocotyls, petioles of cotyledons, and vascular tissue of old leaves, and *prDRG2* was preferentially expressed in sepals, petals, silique walls, and trichomes. We previously found that pea and *Arabidopsis DRG2* transcripts accumulated preferentially in tissues and organs defined to be in a growing state. Here we see that the *DRG1* and *DRG2* promoters are very active in root apices at several stages of development (fig. 2*m*–2*r*). However, neither promoter was active in the shoot apex region of seedlings (fig. 2*k*, 2*l*).

There are many further avenues to pursue regarding *DRG* function. Although steady state levels of *DRG1* and *DRG2* proteins change little in response to most stress conditions (fig. 6), the activity of these proteins could be regulated by posttranslational modifications, subcellular localization, altered rates of synthesis and/or degradation, or other means. *Arabidopsis DRG2* occurs in punctate organelles or granules (Etheridge et al. 1999), but the identity of these granules in not known, nor are the conditions that might cause *DRG*s to associate with them. Although *DRG*s contain all of the sequence motifs that are hallmarks for GTP binding and hydrolysis, GTP binding has been demonstrated experimentally only for *DRG1* from mouse and *Drosophila* (Sazuka et al. 1992*b*; Sommer et al. 1994). GTP-binding properties of plant *DRG1* proteins have not been documented, nor have the binding properties of *DRG2* from any organism. OBGs, bacterial G proteins that are closely related to *DRG*s, provide many useful paradigms for analyzing *DRG* function. For example, OBGs are essential for cell viability, are involved in stress signaling, and physically interact with ribosomes (Kobayashi et al. 2001; Buglino et al. 2002; Lin et al. 2004; Czyz and Wegrzyn 2005; Foti et al. 2005). *DRG2* (or *DRG3*) appears to be involved in heat stress responses. We are testing whether *DRG*s interact with ribosomes, which might then alter translation in some manner. *Xenopus DRG*s interact with DFRPs (Ishikawa et al. 2005). *Arabidopsis* contains apparent homologues of these DFRPs, so we are interested in knowing whether and how these and other proteins interact with plant *DRG*s.

Acknowledgments

The λ genomic library CD4–8 and *DRG1* cDNA clone M70O01 were obtained from the Arabidopsis Biological Re-

source Center. I am grateful to Dr. Scott Grayburn, director of the DNA Core Facility, for DNA sequencing and especially for carrying out qRT-PCR reactions; to Michelle Devitt for technical help during early phases of this work; and to Benjamin Nelson for comments on the manuscript. This research was supported by NIH/AREA grants R15GM54276-1 and R15GM54276-2 and by the Plant Molecular Biology Center, Northern Illinois University.

Literature Cited

Bechtold N, G Pelletier 1998 *In planta Agrobacterium*-mediated transformation of adult *Arabidopsis thaliana* plants by vacuum infiltration. Methods Mol Biol 82:259–266.

Beeckman T, G Engler 1994 An easy technique for the clearing of histochemically stained plant tissues. Plant Mol Biol Rep 12:37–42.

Bischoff F, A Molendijk, CS Rajendrakumar, K Palme 1999 GTP-binding proteins in plants. Cell Mol Life Sci 55:233–256.

Bourne HR, DA Sanders, F McCormick 1990 The GTPase superfamily: a conserved switch for diverse cell functions. Nature 348: 125–132.

——— 1991 The GTPase superfamily: conserved structure and molecular mechanism. Nature 349:117–127.

Buglino J, V Shen, P Hakimian, CD Lima 2002 Structural and biochemical analysis of the Obg GTP binding protein. Structure 10:1581–1592.

Caldon CE, P Yoong, PE March 2001 Evolution of a molecular switch: universal bacterial GTPases regulate ribosome function. Mol Microbiol 41:289–297.

Callis J, M Fromm, V Walbot 1987 Introns increase gene expression in cultured maize cells. Gene Dev 10:1183–1200.

Clemons DJ, C Besch-Williford, EK Steffen, LK Riley, DH Moore 1992 Evaluation of a subcutaneously implanted chamber for antibody production in rabbits. Lab Anim Sci 42:307–311.

Clough SJ, AF Bent 1998 Floral dip: a simplified method for *Agrobacterium*-mediated transformation of *Arabidopsis thaliana*. Plant J 16:735–743.

Craigon DJ, N James, J Okyere, J Higgins, J Jotham, S May 2004 NASCArrays: a repository for microarray data generated by NASC's transcriptomics service. Nucleic Acids Res 32:D575–D577.

Czyz A, G Wegrzyn 2005 The Obg subfamily of bacterial GTP-binding proteins: essential proteins of largely unknown functions that are evolutionarily conserved from bacteria to humans. Acta Biochim Pol 52:35–43.

Devitt ML, KJ Maas, JP Stafstrom 1999 Characterization of *DRG*s, developmentally regulated GTP-binding proteins, from pea and *Arabidopsis*. Plant Mol Biol 39:75–82.

Etheridge N, Y Trusov, JP Verbelen, JR Botella 1999 Characterization of *ATDRG1*, a member of a new class of GTP-binding proteins in plants. Plant Mol Biol 39:1113–1126.

Foti JJ, J Schienda, VA Sutera, ST Lovett 2005 A bacterial G protein-mediated response to replication arrest. Mol Cell 17:1–20.

Ishikawa K, S Azuma, S Ikawa, Y Morishita, J Gohda, T Akiyama, K Semba, J Inoue 2003 Cloning and characterization of *Xenopus laevis DRG2*, a member of the developmentally regulated GTP-binding protein subfamily. Gene 322:105–112.

Ishikawa K, S Azuma, S Ikawa, K Semba, J Inoue 2005 Identification of *DRG* family regulatory proteins (DFRPs): specific regulation of *DRG1* and *DRG2*. Genes Cells 10:139–150.

Jefferson RA, TA Kavanagh, MW Bevin 1987 GUS fusions: β-glucuronidase as a sensitive and versatile gene fusion marker in higher plants. EMBO J 6:3901–3907.

Jones AM, SM Assmann 2004 Plants: the latest model system for G-protein research. EMBO Rep 5:572–578.

Kilian J, D Whitehead, J Horak, D Wanke, S Weinl, O Batistic, C D'Angelo, E Bornberg-Bauer, J Kudla, K Harter 2007 The AtGenExpress global stress expression data set: protocols, evaluation and model data analysis of UV-B light, drought and cold stress responses. Plant J 50:347–363.

Kobayashi G, S Moriya, C Wada 2001 Deficiency of essential GTP-binding protein ObgE in *Escherichia coli* inhibits chromosome partition. Mol Microbiol 41:1037–1051.

Leipe DD, YI Wolf, EV Koonin, L Aravind 2002 Classification and evolution of P-loop GTPases and related ATPases. J Mol Biol 317: 41–72.

Li B, B Trueb 2000 *DRG* represents a family of two closely related GTP-binding proteins. Biochim Biophys Acta 1491:196–204.

Lin B, DA Thayer, JR Maddock 2004 The *Caulobacter crescentus* $CgtA_C$ protein cosediments with the free 50S ribosomal subunit. J Bacteriol 186:481–489.

Mahajan MA, ST Part, XH Sun 1996 Association of a novel GTP binding protein, *DRG*, with Tal1 oncogenic proteins. Oncogene 12: 2343–2350.

Mascarenhas D, IJ Mettler, DA Pierce, HW Lowe 1990 Intron-mediated enhancement of heterologous gene expression in maize. Plant Mol Biol 15:913–920.

Morimoto T, PC Loh, T Hirai, K Asai, K Kobayashi, S Moriya, N Ogasawara 2002 Six GTP-binding proteins of the Era/Obg family are essential for growth in *Bacillus subtilis*. Microbiology 148:3539–3552.

Morrison T, JJ Weis, CT Wittwer 1998 Quantification of low-copy transcripts by continuous SYBR Green I monitoring during amplification. Biotechniques 24:954–962.

Rose AB 2004 The effect of intron location on intron-mediated enhancement of gene expression in *Arabidopsis*. Plant J 40:744–751.

Sazuka T, M Kinoshita, Y Tomooka, Y Ikawa, M Noda, S Kumar 1992*a* Expression of *DRG* during mouse embryonic development. Biochem Biophys Res Commun 189:371–377.

Sazuka T, Y Tomooka, Y Ikawa, M Noda, S Kumar 1992*b* *DRG*: a novel developmentally regulated GTP-binding protein. Biochem Biophys Res Commun 189:363–370.

Schenker T, C Lach, B Kessler, S Calderara, B Trueb 1994 A novel GTP-binding protein which is selectively repressed in SV40 transformed fibroblasts. J Biol Chem 269:25447–25453.

Schmid M, TS Davison, SR Henz, UJ Pape, M Demar, M Vingron, B Schölkopf, D Weigel, J Lohmann 2005 A gene expression map of *Arabidopsis* development. Nature Genet 37:501–506.

Sommer KA, G Petersen, EKF Bautz 1994 The gene upstream of DmRP128 codes for a novel GTP-binding protein of *Drosophila melanogaster*. Mol Gen Genet 242:391–398.

Vernoud V, AC Horton, Z Yang, E Nielsen 2003 Analysis of the small GTPase gene superfamily of *Arabidopsis*. Plant Physiol 131: 1191–1208.

Wolf YI, L Aravind, NV Grishin, EV Koonin 1999 Evolution of aminoacyl-tRNA synthetases: analysis of unique domain architectures and phylogenetic trees reveals a complex history of horizontal gene transfer events. Genome Res 9:689–710.

Yang Z 2002 Small GTPases: versatile signaling switches in plants. Plant Cell 14:S375–S388.

Zhao X-F, PD Aplan 1998 SCL binds the human homologue of *DRG in vivo*. Biochim Biophys Acta 1448:109–114.

Zimmermann P, M Hirsch-Hoffmann, L Hennig, W Gruissem 2004 GENEVESTIGATOR: *Arabidopsis* microarray database and analysis toolbox. Plant Physiol 136:2621–2632.